IECMS
2021

sciforum

Proceedings

Investigating the Effect of Reaction Temperature on the Extraction of Calcium from Ironmaking Slag: A Kinetics Study †

Itumeleng Kohitlhetse [1,*], Kentse Thubakgale [1], Peter Mendonidis [1] and Malibongwe Manono [2]

[1] Department of Metallurgical Engineering, Vaal University of Technology, Private Bag X021, Vanderbijlpark 1911, South Africa; itumelengk@vut.ac.za
2 Centre for Minerals Research, Department of Chemical Engineering, University of Cape Town, Private Bag X3, Rondebosch 7701, South Africa; malibongwe.manono@uct.ac.za
* Correspondence: itumelengk@vut.ac.za; Tel.: +27-016-950-7629† Presented at the title, place, and date.

Abstract: Beneficiation of iron and steel slags have a great potential in mitigating high levels of anthropogenic carbon dioxide (CO2) gas emissions owing to their high contents of calcium and magnesium. Carbonation of calcium and magnesium leaching solutions produce precipitates that promise to act as fluxing agents in various industries. There is also a need to study the physico-chemical factors affecting the extraction of these elements and their kinetic behaviour. A calcium-rich blast furnace ironmaking slag milled to 80% -75µm was used in an experiment to study the effect of reaction temperature on the dissolution of calcium. An orbital shaking incubator was used by applying the one-factor-at-a-time method for a 2-hour leaching test. Reaction temperature was controlled at 30^{0}C, 50^{0}C, 70^{0}C and 100^{0}C at constant agitation speed of 200 rpm, 0.5M of lixiviant concentration and solid-to-liquid ratio kept at 200 g/L. CH3COOH, (NH4)2SO4 and NH4Cl were tested individually as lixiviants. AAS, XRD and EDX were used to analyse the leach filtrate and residue. Consequently, the findings showed that temperature is the critical operating parameter that yielded exceptionally high calcium extraction. CH3COOH yielded 80%-90% of calcium extracted under high reaction temperatures. The kinetic data for the effect of reaction temperature leaching data fitted one shrinking core model equation, which described diffusion-controlled leaching reactions. The diffusion controlled by a product layer model was fitted and the activation energy were calculated as 19.4930 kJ/mol for NH4Cl solvent. (NH4)2SO4 and CH3COOH did not fit into any model because of undefined kinetic data and formation of gelatinous silica layer during leaching process..

Keywords: Ironmaking slag; calcium leaching; reaction temperature; shrinking core models

Citation: Lastname, F.; Lastname, F.; Lastname, F. Title. *Proceedings* **2021**, *68*, x. https://doi.org/10.3390/xxxxx

Published: date

Publisher's Note: MDPI stays neutral with regard to jurisdictional claims in published maps and institutional affiliations.

Copyright: © 2021 by the authors. Submitted for possible open access publication under the terms and conditions of the Creative Commons Attribution (CC BY) license (http://creativecommons.org/licenses/by/4.0/).

1. Introduction

The steel industry is globally the largest energy consuming manufacturing sector and accounts for 7%-12% of anthropogenic greenhouse gas emissions [1]. Measures are hence being developed to improve energy efficiency and reduce CO_2 emissions such as scrap steel recycling, but more drastic measures are needed if reduction goals are to be met in a reasonable timeframe [2]. During manufacturing of iron and steel, a significant amount of about 10%-15% by mass of slag is produced [3]. These materials are made up mainly of CaO, SiO_2, MgO, Al_2O_3 and MnO [4]. The main mineral phases in steel slags are dicalcium and tricalcium silicates, calcium aluminium silicates, calcium oxides and periclase.

Central to the understanding of leaching kinetics are the shrinking core models, namely shrinking core-shrinking particle, shrinking core-constant particle size and shrinking particle, that are regarded as the first types of models developed to describe better heterogeneous and non-catalytic reaction kinetics [5, 6]. According to [7], for chemically controlled reactions the model can be depicted as follows:

$$1-(1-X)^{\frac{1}{3}}=\frac{K_C M_B C_A}{\rho_B \alpha r_0}t= k_r t \tag{1}$$

Consequently, if the kinetics determined by the model seems to be diffusion-controlled, then the equation changes as follows:

$$1-\frac{2}{3}X-(1-X)^{\frac{2}{3}}=\frac{2M_B D C_A}{\rho_B \alpha r_0}t= k_r t \tag{2}$$

Where:

$X=\frac{C}{C_0}$ = Fractional conversion at a given temperature
$K=\frac{K_s C_A}{R_0\,\rho}$ = The apparent rate constant (s^{-1})
K_S = Rate constant of the reaction
ρ_B = Density of the metal extracted (g/ml)
r_0 = Radius of the unreacted particle (m)
C_A = Initial concentration of leachant (mol/ml)
M_B = Molecular mass of metal extracted (g/mol)
D = Diffusion coefficient of the mineral species

[7] also proposed a shrinking core model for solid-liquid controlled leaching reactions. The mathematical expression of the mixed leaching mechanisms is given as [7]:

$$\frac{1}{3}\ln(1-X)+(1-X)^{-\frac{1}{3}}-1=kt \tag{3}$$

Reaction rates are significantly promoted by temperature [8, 9]. The most pronounced observations resulting from this variable is that the temperature must be controlled at all levels if they are to produce reliable kinetic experiments. In addition, a serious consideration of temperature provides crucial information about reaction interaction and mechanisms. Studies by Van't Hoff and Arrhenius were the starting point for all theories of the temperature dependence of reaction rate constants. These observations indicate a close relationship between reaction kinetics and equilibrium constants. The temperature dependence of the equilibrium constant K differs with temperature T, is clearly depicted by the Van't Hoff equation, as indicated in Equations 4 - 7:

$$\frac{dlnK}{dT}=\frac{\Delta H^0}{RT^2} \tag{4}$$

Where:

R = Gas constant (8.314 J/K/mol)

ΔH° = Standard enthalpy change in the reaction

K = Ratio $\frac{K_1}{K_{-1}}$ of the rate constants K_1 and K_{-1} for the forward and reverse reactions.

Similarly:

$$\frac{dlnK}{dT} = \frac{E_a}{RT^2} \tag{5}$$

Where E_a represents the activation energy which corresponds to the standard enthalpy of reaction ΔH° in the Van't Hoff equation. The integral of both sides of the equation with respect to temperature T gives the following product.

$$lnK = lnA - \frac{E_a}{RT} \tag{6}$$

Where lnA is constant of integration with respect to T. The reaction rate constant K is then depicted as follows:

$$K = Ae^{-E_a/RT} \tag{7}$$

A graphical representation of lnK against the inverse of temperature $\left(\frac{1}{T}\right)$ is a linear function that determines the slope $-E_a/R$. Diffusion controlled reactions have an approximate activation energy of less than 21 kJ/mole while reaction and intermediate controlled mechanisms have approximate activation energies of 21 – 40 kJ/mole and 40 – 100 kJ/mole respectively [10, 11, 12].

Authors who have done work on the topic of extraction of calcium from ironmaking slag have highlighted the need for a fundamental insight with regards to mechanisms that govern the leaching of calcium from iron and steel slag [13, 14, 15]. Currently, there is little research information available on the impact of varying physical and chemical parameters during dissolution process of calcium from steel slags. The main objective of this study is to investigate the influence of temperature on the extraction of calcium from the calcium-rich ironmaking slag and thereby establish the reaction-controlling steps during leaching of calcium by using two shrinking core models (SCMs).

2. Materials and Methods

2.1 Materials

A conventional leaching test work was conducted using well-sealed Erlenmeyer flasks rotated in a portable and adjustable orbital shaking incubator. The equipment has the following features: temperature controller, shaker speedometer and shaker timer. Other equipment such as a small-scale rod mill, steel rods, a Jones Riffler sampler, a filter press and an air-compressor were also used. The reagents used for this study include ammonium chloride (NH_4Cl), ammonium sulphate ($(NH_4)_2SO_4$) and acetic acid (CH_3COOH).

2.2 Experimental Procedure

A piece of blast furnace ironmaking slag, 20 mm in size, was blended using a Jones Riffler sampler followed by the dry milling process. The particle size reduction of the sample was achieved using a laboratory scale rod mill for slag particle size reduction down to 80% passing 75 µm. Leaching tests were conducted in 250 ml Erlenmeyer flasks in a portable orbital shaking incubator. For the extraction tests, the slurry was prepared by pouring 20 g of air-dried blast furnace slag powder into the 100 ml pre-conditioned lixiviant solution. The leach slurry agitation rate was maintained at 200 rpm for a period of two hours at temperatures of 30ºC, 50ºC, 70ºC and 100°C. The slurry was then filtered through a 0.2 µm membrane filter placed on the air-supplied filter press. In addition, the amount of filtrate was placed in the 200 ml Erlenmeyer flask for analysis. Approximately 30 ml of filtrate was stored in a 50 ml polyethylene bottle and diluted using a 100x dilution factor for chemical analysis. The filter cake on the membrane filter was dried for 24 hours at 80°C and stored in a vacuum desiccator for material characterisation. A 200 ml bottle of distilled water was used to dilute 2 ml of the filtrate for each lixiviant and their corresponding concentrations. 10 ml of the diluted leach liquor from each lixiviant was used in determining the after-leach results using the atomic absorption spectrometry) (AAS) analyser.

2.3 Characterisation Techniques

2.3.1 Atomic Absorption Spectroscopy (AAS)

Leaching liquor samples were analysed by Varian AAS (AA140) to identify the chemical composition of the leached metals. Standard samples of calcium were prepared at concentrations of 5 ppm, 10 ppm, 20 ppm and 40 ppm in order to identify whether analysis made are in correspondence. Acetylene was used as the fuel for the burner and air as the supporting oxidant. Operational conditions for analysis of calcium were set accordingly. Calcium cathode lambs were also used to detect the concentration of ion metals in the samples. Highly concentrated samples were diluted to be able to be read within the maximum range of the AAS.

2.3.2 X-Ray Diffractometer (XRD)

A Bruker D8 advance powder X-ray diffractometer (XRD) was used to analyse the crystallographic structure of the blast furnace slag using Ca filtered Cu $K\alpha$ radiation at 40 kV and 40 mA. The specimens were scanned at a scan speed of 0.1 s/step in the 2θ range of 5 to 100° at ambient temperature. The phases were identified using X Pert High Score Plus software.

2.3.3 Energy-Dispersive X-Ray Spectrometry (EDX)

Leach residues were analysed by using an EDX spectrometry. EDX is a chemical micro-analysis technique normally used in together with Scanning Electron Microscopy (SEM). The components of this instrument include a sensitive X-Ray detector, a liquid nitrogen is for cooling and a suitable software to collect and provide the readings for the energy spectra.

3. Results

The percentage of calcium extracted increased from about 40% at 30% to about 90% at 100ºC when ammonium chloride was used as the lixiviant (Figure 1). Similarly, with acetic acid the percentage calcium extracted increased from about 60% at 30ºC to about 100% at 100ºC (Figure 1). On the other hand, with ammonium sulphate, calcium extraction remained low (<20%) at all temperatures.

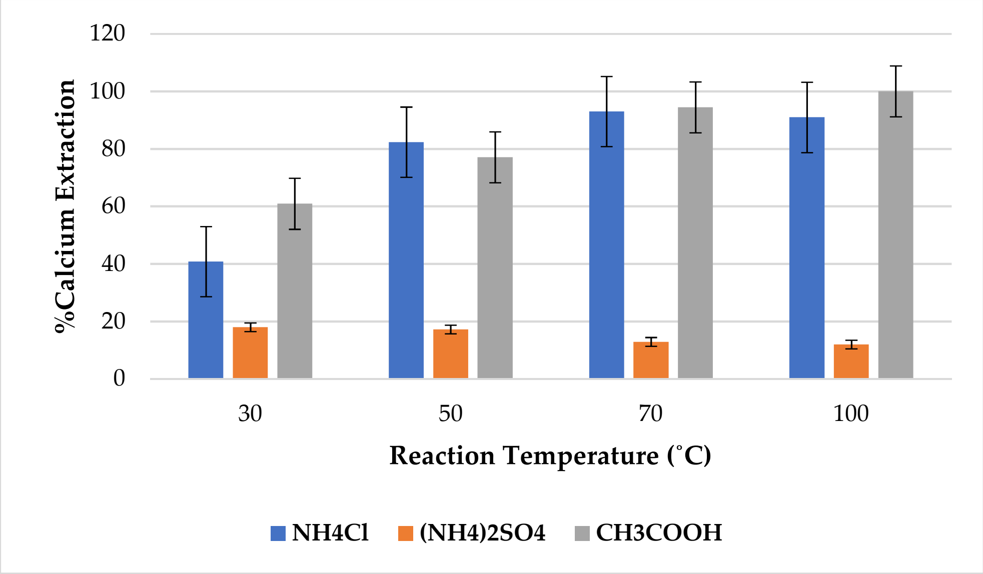

Figure 1: The effect of reaction temperature on the extraction of calcium

Figure 2 represents residue XRD patterns for 0.5 M NH_4Cl, CH_3COOH and $(NH_4)_2SO_4$ leached at 100°C. The final characterisation results show that most of the calcium present is in the form of an aluminoakermanite ($(Ca,Na)_2(Al,Mg,Fe^{2+})$) phase and not composed of the majority of calcium silicates found in previous studies [22]. There are some traces of metallic nickel as well as niobium and titanium enclosed in the form of $NbTi(OH)_3$. All three lixiviants were found to have similar minerals encapsulated in their leach residue but at different quantities as indicated by the peak intensities varying from one lixiviant to another. When CH_3COOH was tested at 0.5 M ionic strength it was found that the aluminoakermanite had lower intensity than those of NH_4Cl and $(NH_4)_2SO_4$.

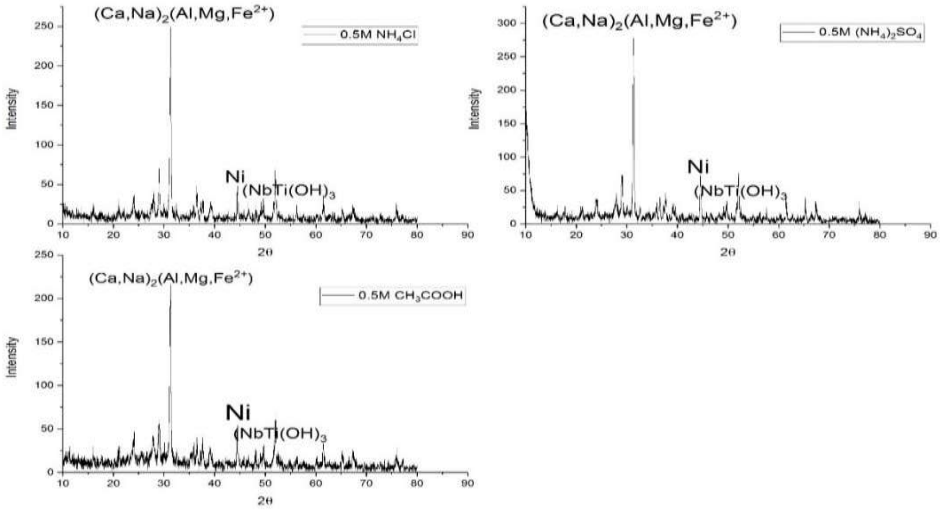

Figure 2: Residue XRD patterns for 0.5 M NH_4Cl, CH_3COOH and $(NH_4)_2SO_4$ leached at 100°C

EDX spectrum analysis was performed on $(NH_4)_2SO_4$, NH_4Cl and CH_3COOH slag residue samples of 0.5 M leached at 100°C. Figure 3 shows that CH_3COOH solvent dissolved calcium significantly as there was only traces of calcium (Ca) in the slag residue. Other peaks shown in Figure 3 are those of potassium (K), manganese (Mn), oxygen (O), magnesium (Mg), aluminium (Al), silicon (Si), lead (Pb) and phosphorus (P). Figure 4 represents the EDX spectrum of slag residue from the NH_4Cl 0.5 M solution leached at 100°C. The slag residue consists of calcium occurring in three peaks with varying spectrum counts. In addition, there are also elements such as K, Mn, O, Mg, Al, Si and Pb. Ammonium sulphate ($(NH_4)_2SO_4$) was found to be less efficient in dissolving calcium from its bearing slag in all variables experimented in this study. Figure 5 display slag residue of $(NH_4)_2SO_4$ at 0.5 M leached at 100°C. The EDX spectrum peaks for $(NH_4)_2SO_4$ are similar with NH_4Cl with slightly different peaks of various elements.

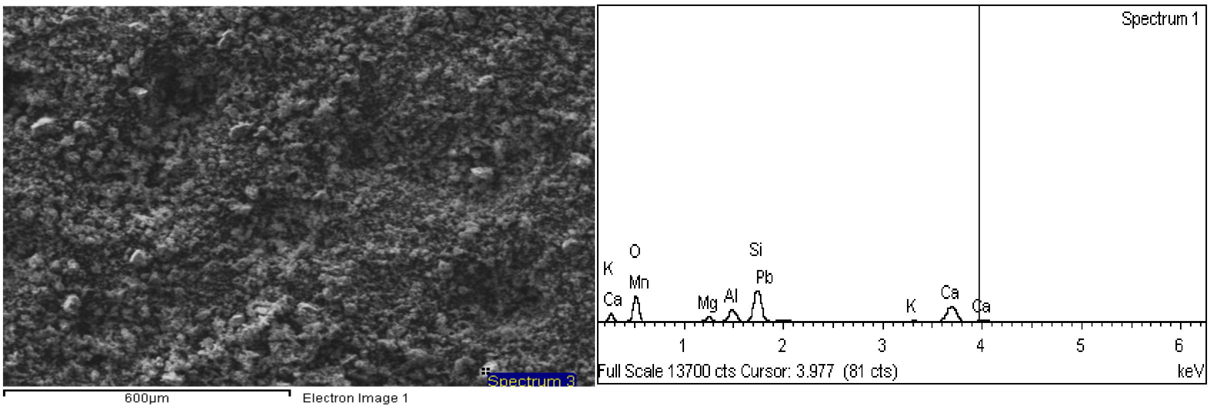

Figure 3: Residue EDX image of 0.5 M CH_3COOH leached at 100°C

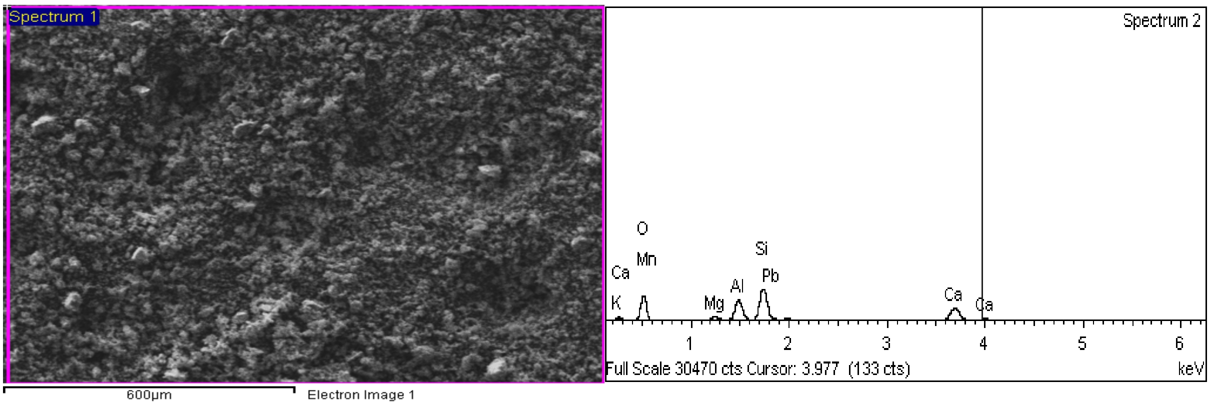

Figure 4: Residue EDX image of 0.5 M NH_4Cl leached at 100°C

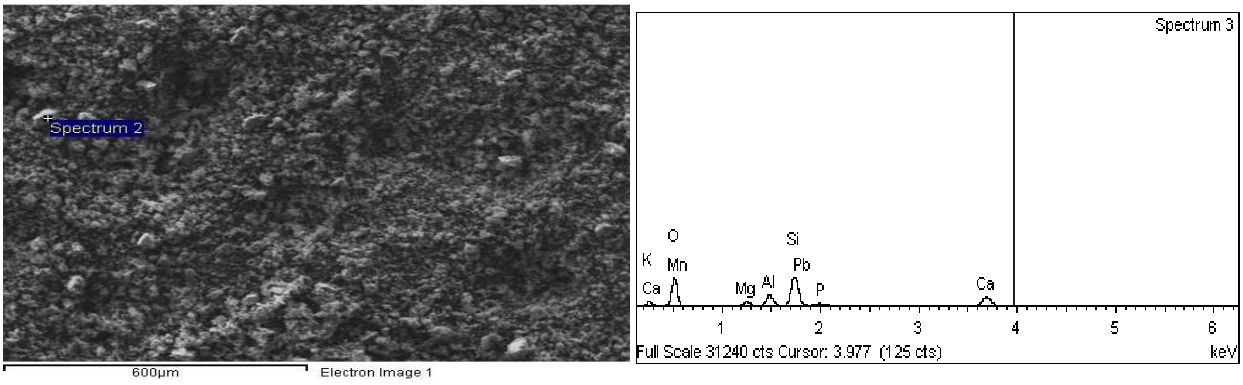

Figure 5: EDX image of 0.5M $(NH_4)_2SO_4$ ionic strength and 120 minutes time

Pearson correlation coefficients (R^2) for NH_4Cl data are displayed by Figure 6 and Figure 7 respectively. It was observed that the increase in R^2 was influenced by the increase in reaction temperature for both chemical and diffusion-controlled mechanisms. There was a significant increase of R^2 from 30°C to 50°C for both mechanisms and is a sudden and insignificant drop in the correlation coefficient as the temperature further increased to 100°C. The results on R^2 when NH_4Cl was tested as a solvent do not fully concur with those of [10] because there is a sudden drop on the Pearson correlation coefficients at temperatures above 50°C. Although, there is no concurrence on temperatures above 50°C particularly on Blast Furnace (BF) ironmaking slag. This may be because the slag behaves differently as compared to natural ores that were previously studied.

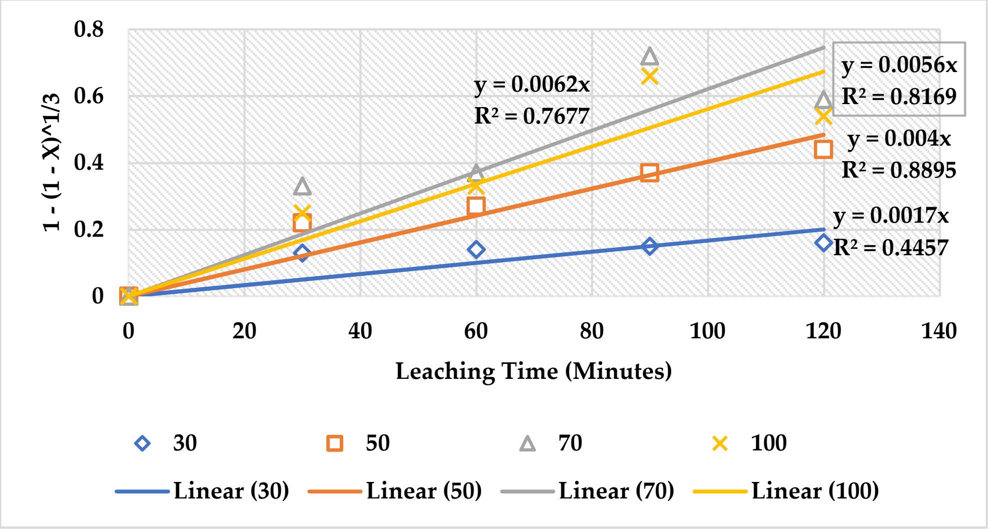

Figure 6: Chemical reaction-controlled mechanism for NH_4Cl solvent

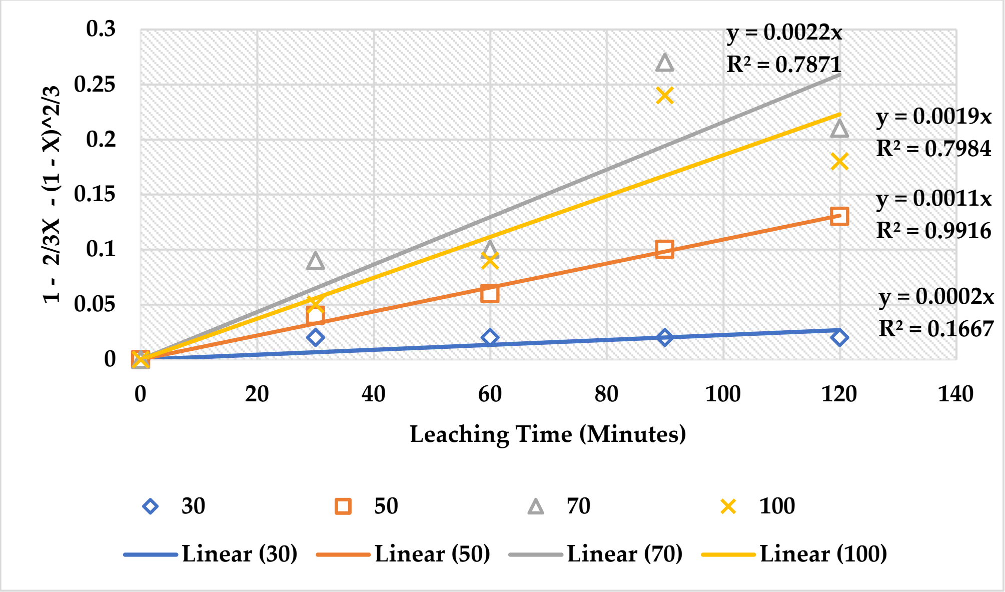

Figure 7: Diffusion controlled mechanism for NH_4Cl solvent

Figure 8 represents the Arrhenius plot for chemical reaction-controlled mechanism in NH_4Cl solvent. The Pearson correlation coefficient (R^2) for the chemically controlled mechanism is 0.126. The value of R^2 that is far less than 0.9 are considered to be indicative of an activation energy that does not correlate with any of the shrinking core models [10]. The calculated activation energies (E_a) from the Arrhenius graphs, where chemical reaction controlled and diffusion-controlled models were plotted and were calculated as 4.8504 kJ/mol and 19.4930 kJ/mol respectively. The R^2 of 0.126 and an activation energy of 4.8504 kJ/mol confirmed that chemically controlled model does not influence the reaction on the dissolution of calcium from ironmaking slag.

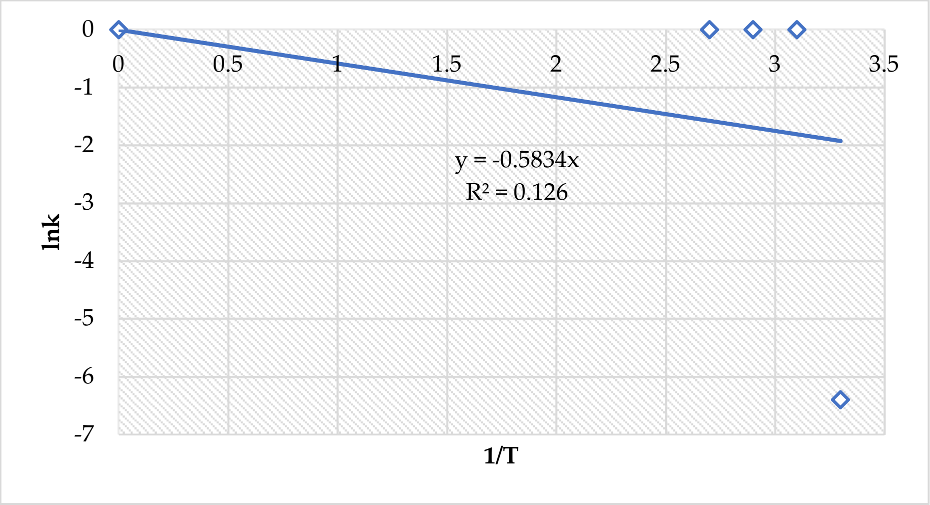

Figure 8: Arrhenius plot for chemical reaction controlled in NH_4Cl solvent.

Figure 9 is an Arrhenius plot for diffusion-controlled mechanism. The R^2 value of 0.9701 and the activation energy of 19.4930 kJ/mol confirmed that the rate-controlling step of NH_4Cl solvent is diffusion by product layer.

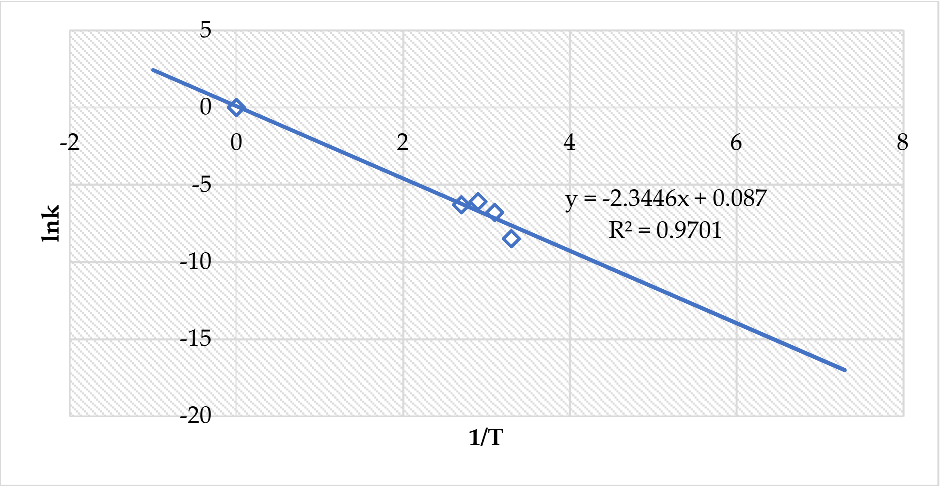

Figure 9: Arrhenius plot for diffusion-controlled mechanism in NH_4Cl solvent.

Pearson correlation coefficients (R^2) for $(NH_4)_2SO_4$ solvent data are shown on Figure 10 and Figure 11. Both chemical reaction and diffusion-controlled mechanisms showed a consistence with the increase in R^2 as the reaction temperature increased. At 30⁰C no reaction mechanism was taking place as there was no R^2 value for all the reaction data fitted in chemical reaction, diffusion and mixed mechanism. The increase in reaction temperature from 50⁰C to 100⁰C resulted in a constant increase in R^2 for both chemical reaction and diffusion-controlled models.

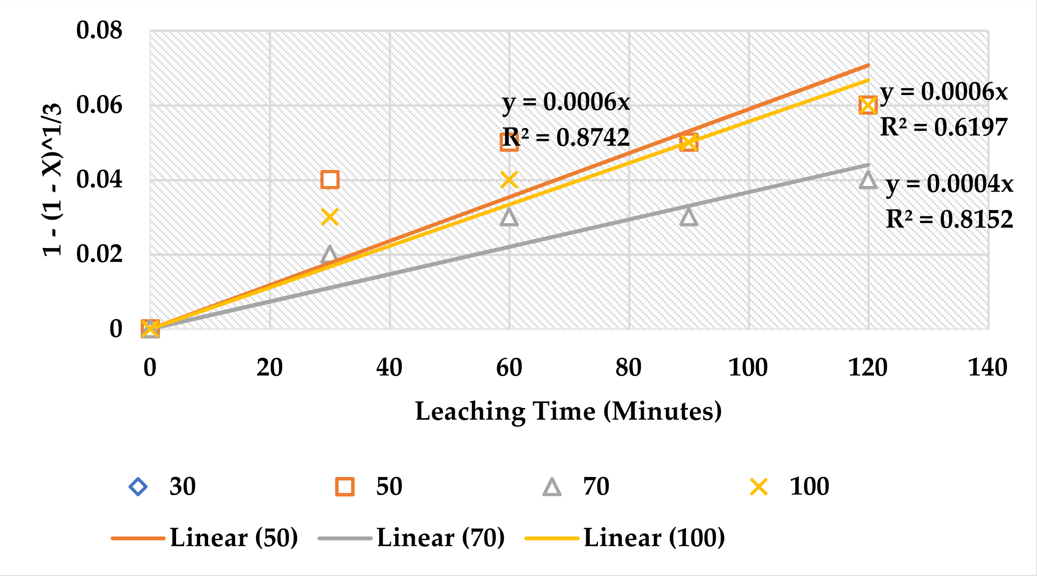

Figure 10: Chemical reaction-controlled mechanism for $(NH_4)_2SO_4$ solvent.

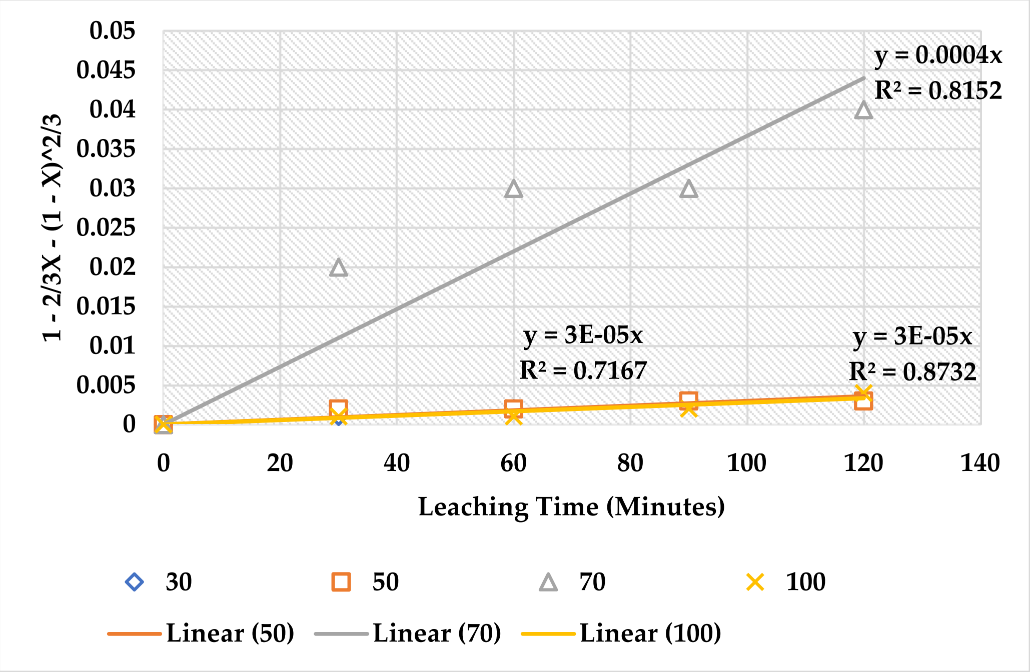

Figure 11: Diffusion controlled mechanism for $(NH_4)_2SO_4$ solvent.

In Figure 12 the activation energy that was determined by chemically controlled mechanism is 2.1234 $kJmol^{-1}$ and it was found to be below the range of any model fitted. In addition, both R^2-value from the Arrhenius plot as well as the activation energy confirm that the dissolution of calcium by $(NH_4)_2SO_4$ is not controlled by the chemical reaction. Furthermore, Arrhenius plot for diffusion-controlled mechanism was graphically undefined.

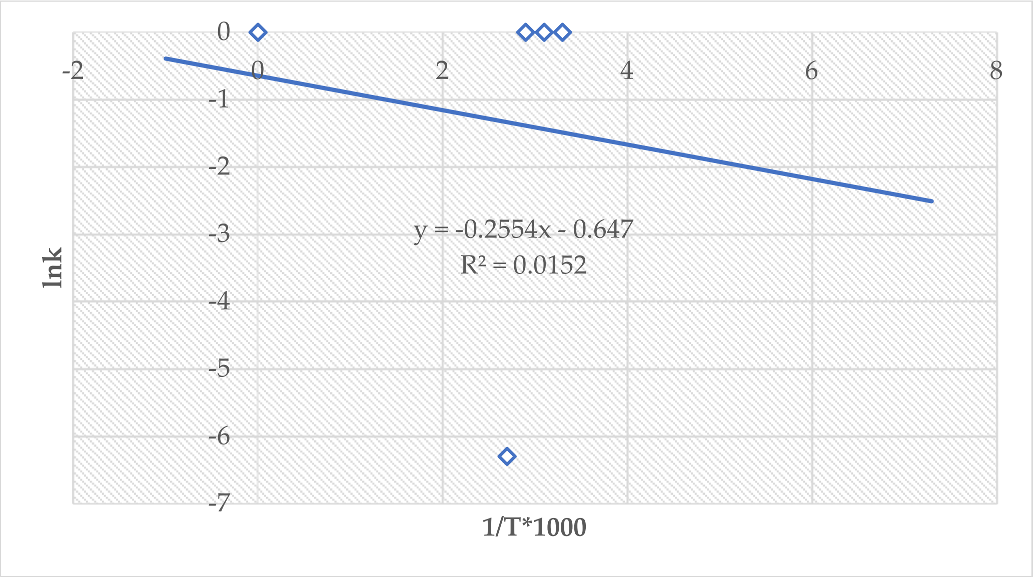

Figure 12: Arrhenius plot for chemically controlled mechanism in $(NH_4)_2SO_4$ solvent

Pearson correlation coefficients (R^2) for the dissolution rates of calcium from ironmaking slag with CH_3COOH used as a solvent were obtained from the data depicted in Figures 13 and 14. The reaction temperature is the most important variable in chemical reactions. There is a trend in the improvement of R^2 with increase in reaction temperature from 30⁰C to 70⁰C for both chemical and diffusion-controlled mechanisms, but the values of R^2 dropped significantly at 100⁰C. The drop in R^2 at 100⁰C is attributed to the formation of silica gel that was reported from experiments where CH_3COOH solvents were used at high temperatures[18, 22].

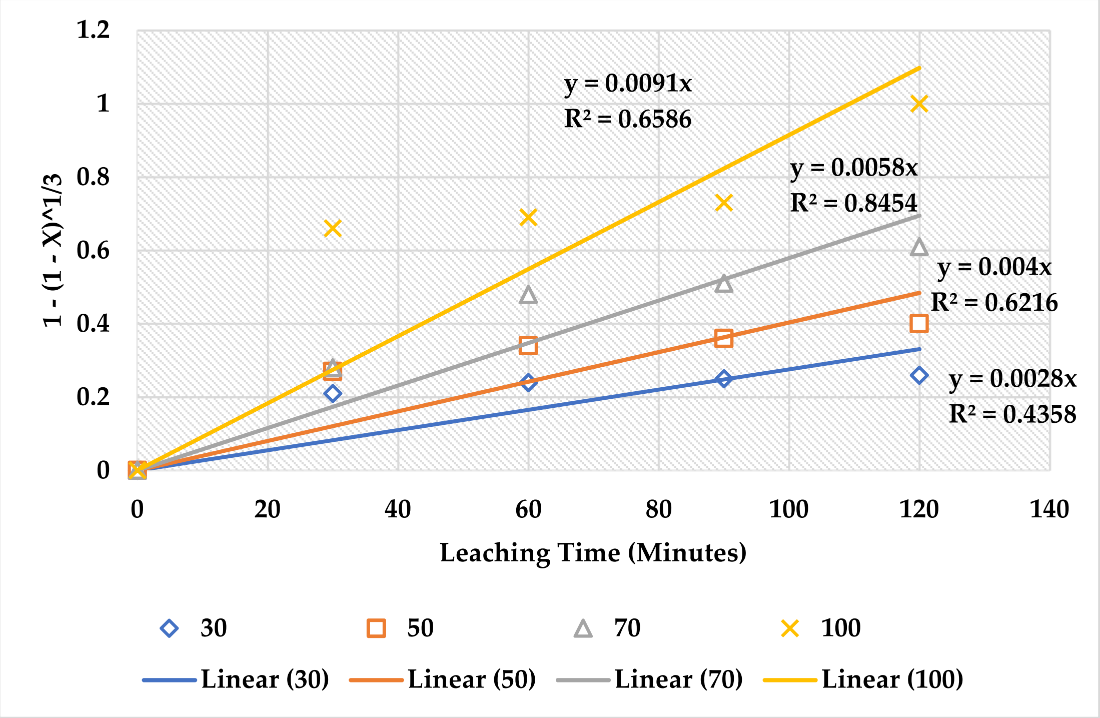

Figure 13: Chemical reaction-controlled mechanism for CH_3COOH solvent.

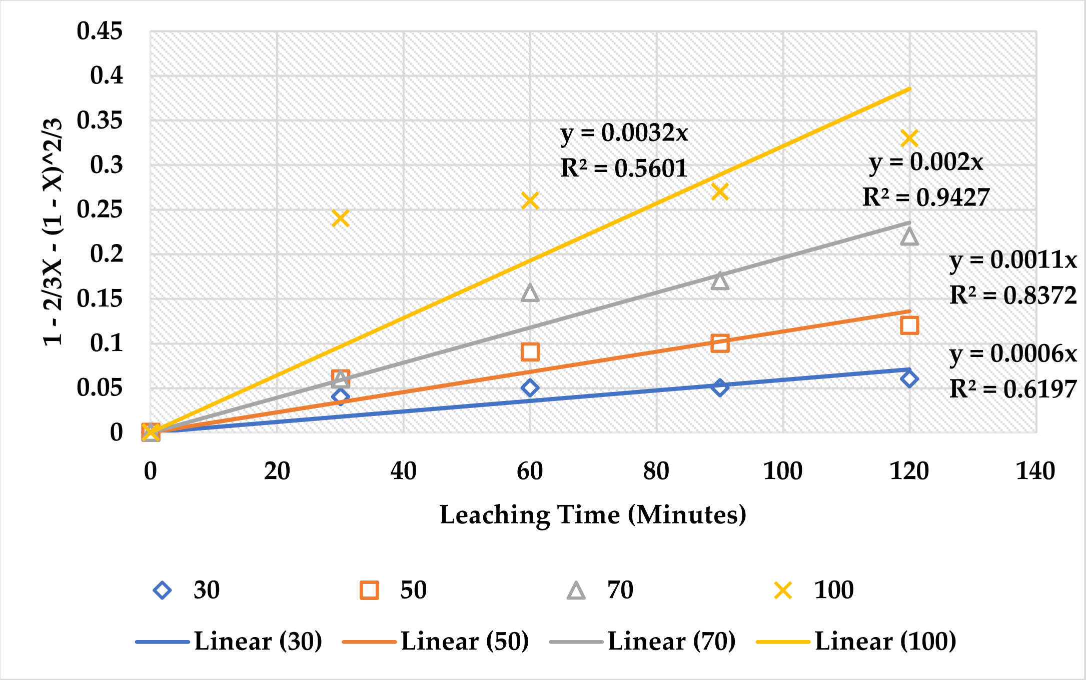

Figure 14: Diffusion controlled mechanism for CH_3COOH solvent

4. Discussion

4.1 The effect of reaction temperature on the extraction calcium from ironmaking slag

Figure 1 displays the influence of increasing the temperature of a leaching incubator to 30˚C to observe the change in calcium recovery. All three lixiviants possessed slight linear curves at different standpoints of calcium recovered in a 30-minute interval leaching reaction of a maximum of 120 minutes. $(NH_4)_2SO_4$ could extract only 18% of calcium in a period of 120 minutes while NH_4Cl reached a peak at 42%. Consequently, CH_3COOH and NH_4Cl had a significant effect on the dissolution of calcium at a reaction temperature of 30˚C by achieving a peak point at 62%.

Regardless of the lixiviant ionic strength, calcium recovery is altered significantly by acidity of the lixiviant [5]. A weak base performed exceptionally well as compared to basic ammonium salts. This is supported by the similarities in calcium recovery in this experimental work and the literature. Acidic leaching environments seemed to give a promise of dissolving calcium, irrespective of residence time, ionic strength, or solid-liquid ratio [8]. In addition, dissolution of calcium by $(NH_4)_2SO_4$ and NH_4Cl as lixiviants is possible at low temperatures (e.g., 30˚C).

NH_4Cl could attain reasonable calcium extraction percentage with increasing dissolution temperatures. $(NH_4)_2SO_4$ has shown that it remains the weakest among the selected lixiviants at 30°C reaction atmosphere. Several studies were conducted on temperature range above the standard state [17, 18, 19], and it has been , it has been shown that temperature influences the extraction efficiencies, particularly on BOS, SS and HMD slags. The temperature of range 30°C to 70°C with aqueous solutions of ammonium acetate and ammonium chloride increases the calcium dissolution efficiency under increased temperatures. In addition, calcium extraction from steel converter and HMD slags from ladle slag were tested with using acetic acid and ammonium salts at 30°C [7]. The present study, using blast furnace slag has shown similarities in calcium dissolution with other types of feedstocks reported in the literature [1]. In all cases calcium leaching was greatly influenced by the chemical composition of slag and enhanced temperature increase.

A 50°C leach temperature is compared with the calcium recovery from calcium-rich slag. The rate at which the reaction temperature was increased resulted in a significant decrease in calcium dissolution by $(NH_4)_2SO_4$ as it resulted in 18% of calcium recovery after 120 minutes of leaching time. On the other hand, CH_3COOH and NH_4Cl achieved 75% recovery after 90 minutes of leaching time. [16] and [20] both experimented with temperature as the factor affecting the reaction rate under the same condition and an average of 65% and 60% calcium recovery was achieved respectively when using CH_3COOH as the solvent. Similarly, the present study deduced a potential of about 76% calcium recovered by CH_3COOH after 120 minutes of leaching reaction suggesting that the current method was more efficient.

Correlations of calcium extraction capability at 70°C were reported by [16] and [20]. Both studies achieved an average calcium recovery of 70% under similar conditions to the present study. These studies were aimed at determining the influence of weak acid CH_3COOH on the dissolution rate of calcium from its feedstock. With temperature increase, the rate of calcium dissolution capability for $(NH_4)_2SO_4$ decreased significantly over the entire leaching period (Figure 1). This trend was continuous from lower temperatures of 30°C and 50°C, which further supports the contention that sulphate ions weaken with increasing reaction temperature. As for NH_4Cl, the calcium recovery increased significantly as the reaction temperature was elevated. As a result, the increase in temperature has a positive influence in NH_4Cl to dissolve calcium over the entire 30-minute interval-leaching period of the maximum residence time of 120 minutes. Meanwhile, elevated incubator temperatures have shown similar dissolution trends in the range of 50°C to 70°C for both NH_4Cl and CH_3COOH. In addition, the NH_4Cl became active in dissolving calcium from blast furnace slag earlier than CH_3COOH especially after 90 minutes of calcium dissolution process. However, calcium recovery dropped significantly after 90 minutes when considering NH_4Cl as a solvent. It could be deduced from this that the maximum leaching recovery of calcium by NH_4Cl was achieved after 90 minutes and decreased drastically during the last dissolution time interval. Calcium dissolution by the CH_3COOH solution kept increasing insignificantly in the last interval whilst NH_4Cl was decreasing, until they both had an equal recovery after the maximum dissolution time. Furthermore, longer leaching periods could result in higher extraction efficiencies [21].

At a temperature of 100°C, there was an observation that 100% of calcium can be extracted from ironmaking slag after a maximum leaching period of 120 minutes. This was only accomplished by CH_3COOH and NH_4Cl whereas, $(NH_4)_2SO_4$ performed poorly at all temperature operating conditions. In addition, silica gelling was also observed at a temperature of 100°C. Silica gelling only formed with CH_3COOH solutions. Furthermore, solid-liquid separation was somewhat hindered but calcium recovery seemed not to be compromised given the fact that this lixiviant was found to be the best in dissolving calcium from the slag.

4.2 XRD analyses of blast furnace ironmaking slag leaching residues

The residue XRD patterns indicated that aluminoakermanite ($(Ca,Na)_2(Al,Mg,Fe^{2+})$) and $NbTi(OH)_3$ were the dominant phases after the leaching process. Many iron and steel slags are made up mainly of CaO, SiO_2, MgO, Al_2O_3 and MnO [3]. The main mineral phases in steel slags are dicalcium and tricalcium silicates, calcium aluminium silicates, calcium oxides and periclase [5]. The findings from this study did not show any common mineral phases with that of the literature and this could be the fact that slags are very reactive and they are capable of changing properties during leaching.

4.3 EDX analyses of blast furnace ironmaking slag leaching residues

EDX spectrum analysis that was performed gives an indication that calcium is present in different forms. There are still peaks of calcium present in the residue and this can better indicate that calcium is was still available as free lime or as solid solutions. In addition, there is no relevant EDX spectrum analyses investigated on the same ironmaking slag to concur this findings in the literature reviewed.

4.4 The effect of reaction rate-controlling mechanisms on the leaching of calcium from ironmaking slag.

To compare with the previous work [10] found that an activation energy of a chemically-controlled process is usually greater than 41.8 kJ/mol while for diffusion-controlled reactions E_a is generally within the range of 4.18 – 12.55 kJ/mol. In addition, [11] suggested that the reaction depends on the diffusion by the product layer when the activation energy is between 8.37 – 20.92 kJ/mol whereas [12] reported figures of 12.55 – 25.08 kJ/mol. The results obtained from this study concur with the findings from [12]. There is a wide range of findings from previous work on reaction-controlling mechanisms; this is because there is also a wide range of experimental conditions and leaching variables. In some cases leaching reactions were assisted by catalysts, while others are run with unassisted and/or blended solvents. Nonetheless, the activation energies obtained in the present work confirmed that leaching of calcium from CaO bearing slag was controlled by diffusion by the product layer since they fall in the range of 12.55 – 25.08 kJ/mol.

During leaching with $(NH_4)_2SO_4$ solvent, low recoveries of calcium were observed from analyses. Similar problem has been previously observed with the diffusion-limiting silica (SiO_2) layering in silicate minerals such as serpentine [23]. The main reason for the low dissolution of calcium and magnesium from silicate minerals by reaction mechanisms is the increase of particle radius due to increasing silica-rich layer that remains passive during leaching reaction [6]. Therefore, the ordinary shrinking core model does not apply due to formation of silica gelatinous layer. In order to correct the model prediction, two-stage leaching is sometimes used to decrease silica gelling that core the core of the mineral [24]. High-silica content on the blast furnace slag consequently created resistance to calcium extraction when $(NH_4)_2SO_4$ solvents were used.

Although CH_3COOH solvents attained high recoveries of calcium with increasing temperature, thick SiO_2 gelatinous layer in the residue was observed after the leaching reaction. Filtration process efficiency was also affected by the silica layer. Arrhenius plots for chemically and diffusion-controlled mechanisms during fitting in CH_3COOH solvent kinetic data were also graphically undefined, similar to the $(NH_4)_2SO_4$ diffusion model. The recovery of calcium indicates that the rate-limiting step of dissolution of the dominant mineral in the ironmaking slag (aluminoakermanite) in CH_3COOH is most likely due to formation of a passive silica layer. The silica-rich layer remains passive during dissolution of magnesium and calcium from silicate minerals [23].

Mixed reaction, chemical reaction and diffusion-controlled mechanisms have no importance in interpreting the leaching rates of calcium when CH_3COOH and $(NH_4)_2SO_4$ were used as lixiviants due to the formation of silica layer. The leaching behaviour high-silica minerals such as wollastonite and serpentine are sometimes dissolution rates, where kinetic models are inappropriate [6]. Nevertheless the rate-controlling steps of the leaching reaction is influenced by increase in size of the particle radius at high temperatures. The dissolution rate of calcium and magnesium can still increase over time [24]. Consequently, leaching still took place and CH_3COOH lixiviant showed best leaching results in calcium dissolution, despite the failure to generate reasonable kinetic data. Selective flotation of quartz and multi-stage leaching of high-silica minerals that are rich with calcium and magnesium were previously investigated [24]. However, selective separation of free quartz did not eliminate the problem of the formation of gelatinous silica layer during leaching of calcium and magnesium [23].

5. Conclusions

The experimental results from this study show that extraction of calcium from ironmaking slag by leaching is feasible. The best calcium recovery was achieved by acetic acid; ammonium salts were less efficient. 100% extraction can be achieved with a solid-liquid ratio of approximately 200 g/L, reaction temperatures of 100˚C and 0.5 M acetic acid. As the reaction temperature was increased from 50˚C up to 100˚C, silica gelling was observed, which hindered filtration of a leach liquor from a residue. Silica gelling did not compromise calcium recovery, but it appears to have affected the reaction rates. The XRD analyses of the leach residue showed high concentrations of calcium in the form of silicates, also known as aluminoakermanite ($(Ca,Na)_2(Al,Mg,Fe^{2+})$). EDX analysis of the residue also deduced that there is free calcium present in the ironmaking slag that was investigated. The kinetic data for the effect of reaction temperature leaching data fitted the shrinking core model equation, $1 - 2/3x - (1 - x)^{2/3}$, which described diffusion-controlled leaching reactions. The diffusion controlled by a product layer model was fitted and the activation energy was calculated as 19.4930 kJ/mol for NH_4Cl solvent. The kinetic data for $(NH_4)_2SO_4$ and CH_3COOH solvents did not fit into any model because of formation of gelatinous silica layer during leaching process.

References

1. Cloete, M. 2010. Atlas on geological storage of CO_2 in South Africa. Council for Geosciences. Pretoria, South Africa.
2. Robie, R.A., Hemingway, B.S., Fischer, J.R., 1978. Thermodynamic properties of minerals and related substances at 298.15K and 1 bar (105 Pa) pressure and at higher temperatures. *US Geol. Bull. 1452*.
3. Fehling, K.A., Proctor, D.M., Shay, E.C., Wittenborn, J.L., Green, J.J., Avent, C., Bigham, R.D., Connolly, M., Lee, B., Shepker, T.O., Zak, M.A., (2000). Physical and chemical characteristics of blast furnace, basic oxygen furnace and electric arc furnace steel industry slags. *Environ. Sci. Technol. 34 (2000) 1576–1582.*
4. Garrels, R. M., & Christ, C. L., (1990). Solutions, Minerals, and Equilibria. Boston, London, United Kingdom: Jones and Bartlett Publishers.
5. Levenspiel, O., (1999). Chemical Reaction Engineering, *third edition. Wiley*, New York.
6. Othusitse, N., Muzenda, E., (2015). Predictive models of leaching processes: A critical review. *7th international conference on latest trends in engineering and technology*, pp. 136 – 141.
7. Dickinson, C.F. & Heal, G.R. (1999). Solid-liquid diffusion-controlled rate equations. *Thermochimica Acta 340 – 341(0): 89 – 103.*
8. Radingoana, P.M., (2014). Leaching of low-grade laterite ore from waterval mine in Mpumalanga through electrochemical process. *Magister Technologiae Dissertation*, Tshwane University of Technology, South Africa.
9. Thubakgale, C.K., (2013). Leaching and recovery of nickel and cobalt from the waterval boven laterite ore. *Magister Technologiae Dissertation*, Tshwane University of Technology, South Africa.
10. Habashi, F., (1999). Kinetics of metallurgical process. Metallurgie Extractive, Quebec, Quebec City Canada.
11. Anand, S., Das, S.C., Das, R.P. & Jena, P.K. 1988. Leaching of manganese nodules at elevated temperature and pressure in the presence of oxygen. *Hydrometallurgy*, 20(2):155 - 167.
12. Romankiw, L.T., De Bruyn, P.L., 1963. Kinetics of dissolution of zinc sulphide in aqueous sulphuric acid. In: WADSWORTH, M., DAVIS, F.T., (Eds.), *Unit Processes in Hydrometallurgy*, 62, Dallas, TX.
13. Sanna, A., Uibu, M., Caramanna, G., Kuusik, R., Maroto-Valer, M.M., (2014). A review of mineral carbonation technologies to sequester CO_2. *Royal Society of Chemistry, UK.*
14. Kotoane, M., (2013). Development and optimisation of selective leaching processes for the extraction for calcium from steel slag in view of sequestering carbon dioxide. *Magister Technologiae Dissertation*, Vaal University of Technology, South Africa.
15. Yogo, K., Teng, Y., Yashima, T., Yamada, K., (2005). Development of a new CO_2 fixation/utilisation process (1): recovery of calcium from steelmaking slag and chemical fixation of carbon dioxide by carbonation reaction. *Greenhouse Gas Control Technol. 7, 2427-2430.*
16. Witkamp, J.J., Huijgen, G – J., Comans, R.N.J., (2005). Mineral CO_2 sequestration by steel slag carbonation. *Environ. Sci. Technol. 39: 9676 – 9682.*
17. Hall, C., Large, D.J., Adderley B., and West H.M., (2014). School of Chemical and Environmental Engineering, University of Nottingham, Nottinham, UK.
18. Mattilla, H-P., Grigaliunaite, I., and Zevenhoven, R., (2012). Chemical kinetics modelling and process parameter sensitivity for precipitated calcium carbonate production from steelmaking slags. *Thermal and Flow Engineering Laboratory*, Abo Akademi University, Piispankuru 8, 20500 Turku, Finland
19. Eloneva, S., Salminen, J., Fogelholm, C., Zevenhoven, R., (2012). Preliminary assessment of a method utilizing carbon dioxide and steelmaking slags to produce precipitated calcium carbonate, *Appl. Energy. 90, 329-334.*
20. Bilen, M., Altiner, M., & Yildirim, M., (2017). Evaluation of steelmaking slag for CO_2 fixation by leaching-carbonation process. *Particulate Science and Technology*, 36:3:368-377.

21. Stange, W., (1998). The process design of gold leaching and carbon-in-pulp circuits. *South African Institute of Mining and Metallurgy (SAIMM)*, Johannesburg, South Africa.
22. Baciocchi, R., Costa, G., Polettini, A. & Pomi, R. 2009. Influence of particle size on the carbonation of stainless-steel slag for CO2 storage. *Energy Procedia,* I:4859-4866.
23. Didyk-Mucha, A., Pawlowska, A., Sadowski, Z., (2016). Application of the shrinking core model for dissolution of serpentine in an acid solution. *Department of Chemical Engineering, Wroclaw University of Technology*, Wybrzeze, 50-370, Poland
24. Sun, Y., Yao, M-S., Zhang, J-P., Yang, G., (2011). Indirect CO_2 mineral sequestration by steelmaking slag with NH_4Cl as leaching solution. *Chem. Eng. J. 173, 437-445.*